

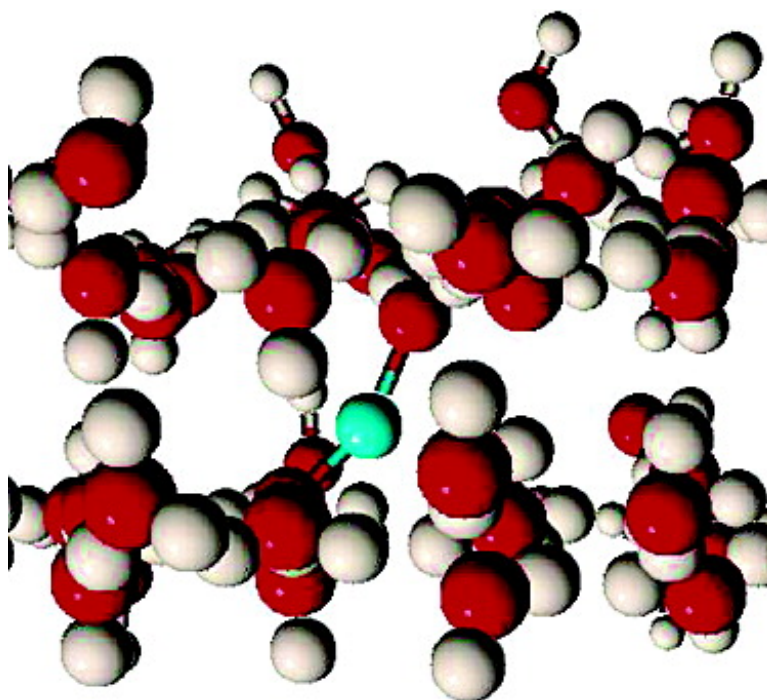
Article

Protons Colliding with Crystalline Ice: Proton Reflection and Collision Induced Water Desorption at Low Incidence Energies

Pepa Cabrera Sanfelix, Ayman Al-Halabi, George R. Darling, Stephen Holloway, and Geert-Jan Kroes

J. Am. Chem. Soc., **2005**, 127 (11), 3944-3951 • DOI: 10.1021/ja040171u • Publication Date (Web): 25 February 2005

Downloaded from <http://pubs.acs.org> on March 24, 2009



More About This Article

Additional resources and features associated with this article are available within the HTML version:

- Supporting Information
- Access to high resolution figures
- Links to articles and content related to this article
- Copyright permission to reproduce figures and/or text from this article

[View the Full Text HTML](#)



ACS Publications
High quality. High impact.

Protons Colliding with Crystalline Ice: Proton Reflection and Collision Induced Water Desorption at Low Incidence Energies

Pepa Cabrera Sanfelix,[†] Ayman Al-Halabi,^{*,†,§} George R. Darling,[†]
Stephen Holloway,[†] and Geert-Jan Kroes[‡]

Contribution from the Surface Science Research Centre, Department of Chemistry,
The University of Liverpool, Liverpool L69 3BX, UK, and Leiden Institute of Chemistry,
Sorlaeus Laboratories, P.O. Box 9502, 2300 RA Leiden, The Netherlands

Received July 15, 2004; E-mail: a.al-rimawi@liverpool.ac.uk

Abstract: We present results of classical trajectory (CT) calculations on the sticking of protons to the basal plane (0001) face of crystalline ice, for normal incidence at a surface temperature (T_s) of 80 K. The calculations were performed for moderately low incidence energies (E_i) ranging from 0.05 to 4.0 eV. Surprisingly, significant reflection is predicted at low values of E_i (≤ 0.2 eV) due to repulsive electrostatic interactions between the incident proton and the surface water molecules with one of their H-atoms pointing upward toward the gas phase. The sticking probability increases with E_i and converges to unity for $E_i \geq 0.8$ eV. In the case of sticking, the proton is trapped in the ice forming a Zundel complex ($H_5O_2^+$), with an average binding energy of 9.9 eV with a standard deviation of 0.5 eV, independent of the value of E_i . In nearly all sticking trajectories, the proton is implanted into the ice surface, with a penetration depth that increases with E_i . The strong interaction with the neighboring water molecules leads to a local rupture of the hydrogen bonding network, resulting in collision induced desorption of water (puffing), a process that occurs with significant probability even at the lowest E_i considered. The probability of water desorption increases with E_i . In nearly all trajectories in which water desorption occurs, a single three-coordinated water molecule is desorbed from the topmost monolayer.

1. Introduction

The interaction between water ice and protons is important to a large range of chemical environments, ranging from the interstellar medium (ISM), planetary surfaces, and comets to our own atmosphere. Proton–ice interaction is relevant to numerous fundamental processes, such as the formation of molecules at surfaces of interstellar grains,^{1,2} ion implantation,³ and water sputtering.⁴ It is also relevant to analytical techniques, such as proton channelling, which can be used to investigate surface disorder of ice.⁵ As a result of their importance, interactions of protons with water ice have been studied both experimentally^{4–7} and theoretically,^{8–10} for a wide range of conditions.

Outside the earth's atmosphere, protons are present in cosmic rays (CRs) that consist of energetic charged particles, mostly

of galactic origin. The CRs can also be generated in the sun and interplanetary space. They consist predominantly of protons (about 90%) and He nuclei (about 10%) with electrons as a minor constituent.¹¹ In the ISM, ice is present as icy mantles of submicron thickness, covering dust grain particles that typically consist of silicate or carbonaceous cores. The structure of interstellar ice is known to be predominantly amorphous,¹² but recent experiments¹³ and astronomical observations^{14,15} also clearly suggest the presence of crystalline ice. The icy mantles also contain other molecules, such as CO, CO₂, NH₃, and CH₄.¹⁶ In such environments, incoming CRs can promote the formation of carbonic molecules such as carbonic acid (H₂CO₃), which was found to form upon exposing H₂O–CO₂ mixtures to high

[†] The University of Liverpool.

[‡] Leiden Institute of Chemistry.

[§] Also known as Ayman Al-Remawi.

- (1) Brucato, J. R.; Palumbo, M. E.; Srazzulla, G. *Icarus* **1997**, *125*, 135.
- (2) Gerakines, P. A.; Moore, M. H.; Hudson, R. L. *Astron. Astrophys.* **2000**, *357*, 793.
- (3) Srazzulla, G.; Leto, G.; Gomis, O.; Satorre, M. A. *Icarus* **2003**, *164*, 163.
- (4) Baragiola, R. A.; Vidal, R. A.; Svendsen, W.; Schou, J.; Shi, M.; Bahr, D. A.; Atteberry, C. L. *Nucl. Instrum. Methods Phys. Res., Sect. B* **2003**, *209*, 294.
- (5) Golecki, I.; Jaccard, C. *J. Phys. C: Solid State Phys.* **1978**, *11*, 4229.
- (6) Brown, W. L.; Lanzerotti, L. J.; Poate, J. M.; Augustyniak, W. M. *Phys. Rev. Lett.* **1978**, *40*, 1027.
- (7) Souda, R. *Curr. Appl. Phys.* **2003**, *3*, 13.

- (8) Brenner, D. W.; Garrison, B. J. *Phys. Rev. B: Condens. Matter* **1986**, *34*, 5782.
- (9) Ohgaito, R.; Hirata, K.; Mukai, T. *Adv. Space Res.* **1999**, *23*, 1235.
- (10) Kobayashi, C.; Iwahashi, K.; Saito, S.; Ohmine, I. *J. Chem. Phys.* **1996**, *105*, 6358.
- (11) Bazilevskaya, G. A.; Krainev, M. B.; Makhmutov, V. S. *J. Atmos. Sol-Terr. Phys.* **2000**, *62*, 1577.
- (12) Hagen, W.; Tielens, A. G. G. M.; Greenberg, J. M. *Chem. Phys.* **1981**, *56*, 367.
- (13) Chakarov, D.; Kasemo, B. *Phys. Rev. Lett.* **1998**, *81*, 5181.
- (14) Malfait, K.; Waelkens, C.; Waters, L. B. F. M.; Vandenbussche, B.; Huygen, E.; de Graauw, M. S. *Astron. Astrophys.* **1998**, *332*, L25.
- (15) Maldoni, M. M.; Egan, M. P.; Smith, R. G.; Robinson, G.; Wright, C. M. *Mon. Not. R. Astron. Soc.* **2003**, *345*, 912.
- (16) Ehrenfreund, P.; Schutte, W. A. Infrared observations of interstellar ices; Minh, Y. C., van Dishoeck, E. F., Eds.; In *Astrochemistry: From Molecular Clouds to Planetary Systems*; IAU, Astron. Soc. Pac.: San Francisco, CA, 2000; Vol. 197, p 135.

energy protons,^{1,2} and of organic molecules, such as amino acids.¹⁷ In addition to chemical reactions, CRs also induce other energetic processes in icy mantles: the CR–ice interaction is the predominant agent leading to mass loss of water-ice grains.¹⁸ Thick deposits of ice (much thicker than the icy mantles of the ISM, and thicker than the CR penetration depth) are present on planetary surfaces and on comets³. Surface implantation of bombarding ions³ is relevant for a variety of processes occurring in these environments.

Cosmic rays and solar protons can penetrate our atmosphere to some extent, thereby affecting atmospheric ion chemistry.^{19–22} The CRs play a significant role in atmospheric processes and phenomena, such as ozone depletion and the green house effect.^{11,23}

In our atmosphere, ice is present at different altitudes. The mesosphere is at heights of more than 80 km, where noctilucent clouds exist. Here, ion water clusters $H^+(H_2O)_n$ exist, which are formed in a chain of events initiated by O_2^+ cations (see ref 24 for the details of the formation mechanism). The formation of these charged clusters is believed to promote the nucleation of neutral water clusters through subsequent dissociative recombination reactions with electrons.²⁴

The stratosphere is at heights between 15 and 50 km. Near the poles at ~ 20 km, polar stratospheric clouds can form in winter time. These clouds, which catalyze ozone destruction, are known to consist of crystalline ice particles.²⁵ The location of these clouds coincides with the altitude at which the intensity of cosmic ray cascades is at its maximum (see ref 26 and references therein). These cascades, also known as secondary cosmic ray particles, are produced by the incidence of cosmic particles upon our atmosphere. They contain muons, protons, and other hadrons. Protons can also reach the upper layer of the troposphere (which extends up to ~ 15 km), where cirrus cloud ice particles are present and may play a role in the depletion of ozone.²⁷

Not only are proton ice interactions important to a variety of chemical environments, they can also be exploited in analytical techniques. For example, proton channelling has been used to investigate surface melting of ice of a few nanometers thickness at different surface temperatures (T_s), at a normal incidence energy (E_i) of 100 keV.⁵

Experiments on proton–ice interactions have been performed for a variety of conditions. Brown et al. studied the interaction of highly energetic (MeV), light ions such as H^+ and O^+ with ice.⁶ The collisions were observed to lead to sputtering, with 0.4 (0.2) H_2O molecules coming off the surface per incident proton at $E_i = 0.5$ (1.5) MeV. The experimentalists believed the water molecules to be ejected stoichiometrically, but they

could not determine whether molecules were ejected as monomers or in clusters. The observation that the sputtering coefficients were independent of the thickness of the ice film suggested that the erosion of the water molecules occurred near the surface–vacuum interface.⁶ Many experiments have been performed afterward on water sputtering by high incident energy ions (see the review of Bariagiola et al.⁴ and references therein). The main conclusions drawn from these experiments agree well with those of the pioneering experiments of Brown et al.⁶

At somewhat lower, but still high proton E_i (100 eV), femtosecond experiments⁷ were performed to study proton scattering and secondary ion desorption (of proton hydrated species) from water ice adsorbed on a Pt(111) surface, at an incidence angle of 20°. At high coverage (> 10 monolayers (ML)), a high sticking probability was found. Only bare protons were observed to scatter at high coverage. Secondary ions ($H^+(H_2O)_n$, $n = 1–10$) were only observed at a low coverage (0.1 ML) and low T_s (15 K).

Proton transfer under equilibrium conditions in H_2O/D_2O amorphous ice mixtures was studied by reactive ion scattering (RIS) experiments for $T_s = 95–140$ K.²⁸ In these experiments, Cs^+ scatters off the surface at $E_i < 35$ eV. The scattered Cs^+ can take one or more water molecules with it, and the presence of HDO (the occurrence of proton exchange) is detected by mass spectrometry. For pure ice films, no exchange of thermally generated protons was observed at low T_s , but proton exchange was observed to occur on a time scale of minutes at $T_s = 140$ K. Addition of HCl to the film to yield excess protons led to quick proton exchange (proton exchange at the surface going to completion within a minute), but the proton exchange was lateral in nature, being confined to the top bilayer at 95 K and to the top three bilayers at 140 K. The experiments suggest that the proton prefers to stay on the surface rather than move into the bulk,²⁸ in agreement with the experimental results of Cowin et al.²⁹

Scattering of protons from ice has also been studied theoretically. A qualitative, classical trajectory (CT) study was performed for protons scattering from an amorphous ice cluster consisting of 100 water molecules, for E_i ranging from high (840 eV) to very low (0.84 meV).⁹ Because very few trajectories were run (up to 5 per E_i), the calculations did not allow quantitative conclusions to be drawn. Interestingly, water sputtering was found to be quite efficient for low E_i (≤ 8.4 eV). However, at the highest E_i , the protons just passed through the amorphous ice cluster, and water sputtering was not observed. In contrast, a CT study of scattering of O^+ from cubic ice, for $E_i = 23–115$ eV, showed the sputtering yield to increase with E_i .⁸ In most trajectories showing water sputtering, the sputtered material consisted of a single intact water molecule.⁸ In those calculations, most of the sputtered molecules (up to 97–99%) originated from the surface–vacuum interface, as suggested by the erosion experiments of Brown et al.⁶ In most cases, the incident O^+ ions were found to be implanted in the surface rather than reflected into the gas phase, with reflection decreasing with increasing E_i . Fragmentation of the surface water molecules upon impact was only observed at the highest energies considered (115 eV).⁸

- (17) Kobayashi, K.; Kasamatsu, T.; Keneko, T.; Koike, J.; Oshima, T.; Saito, T.; Yamamoto, T.; Yanagawa, H. *Adv. Space Res.* **1995**, *16*, 21.
- (18) Mukai, T.; Schwehm, G. *Astron. Astrophys.* **1981**, *95*, 372.
- (19) Tinsley, B. A.; Brown, G. M.; Scherrer, P. H. *J. Geophys. Res., [Atmos.]* **1989**, *94*, 14783.
- (20) Tinsley, B. A.; Deen, G. W. *J. Geophys. Res., [Atmos.]* **1991**, *96*, 22283.
- (21) Tinsley, B. A.; Heelis, R. A. *J. Geophys. Res., [Atmos.]* **1993**, *98*, 10375.
- (22) Besprozvannaya, A. S.; Ohl, G. I.; Sazonov, B. I.; Scherba, I. A.; Schuka, T. I.; Troshichev, O. A. *J. Atmos. Sol-Terr. Phys.* **1997**, *59*, 1233.
- (23) Shumilov, O. I.; Kasatkina, E. A.; Henriksen, K.; Raspopov, O. M. *J. Atmos. Sol-Terr. Phys.* **1995**, *57*, 665.
- (24) Wayne, R. P. *Chemistry of Atmospheres*, 3rd ed.; Oxford University Press: 2000.
- (25) Solomon, S. *Rev. Geophys.* **1999**, *37*, 275.
- (26) Ziegler, J. F. *IBM J. Res. Dev.* **1996**, *40*, 19.
- (27) Zondlo, M. A.; Hudson, O. K.; Prenni, A. J.; Tolbert, M. A. *Annu. Rev. Phys. Chem.* **2000**, *51*, 473.

(28) Park, S.-C.; Jung, K.-H.; Kang, H. *J. Chem. Phys.* **2004**, *121*, 2765.

(29) Cowin, J. P.; Tsekouras, A. A.; Iedema, M. J.; Wu, K.; Ellison, G. B. *Nature (London)* **1999**, *398*, 405.

In explorative calculations, Ohmine and co-workers investigated the dynamics of proton attachment to a water cluster consisting of 64 molecules at $T = 15$ K, using molecular dynamics (MD) simulations.¹⁰ Twenty trajectories were computed for different initial positions of H^+ relative to the cluster. The proton was initially placed at a distance of 15 \AA from the center of the cluster, with zero initial momentum. Following impact, on average 3.8 water molecules desorbed from the cluster on a time scale shorter than 1 ps. During this time, proton transfer from one water molecule to another proceeded over barriers that are lower than the proton's energy, so that classical mechanics can be assumed to hold at this initial stage of the proton-ice interaction. Initially, H^+ was always associated with one water molecule. At the next stage, proton transfer to another molecule proceeded through a Zundel complex, i.e., $(H_5O_2)^+$ solvated by other water molecules, and next to another water molecule, and so on. During the transfer, both water molecules involved in the Zundel complex had to have a low hydrogen bond coordination number (less than 3 hydrogen bonds to other water molecules). The proton transfer was observed to proceed through the anomalous diffusion mechanism, i.e., the proton transferred from a water molecule is often not the one it accepted.

Ohmine and co-workers have also studied proton solvation and proton transfer in cubic ice, in simulations in which they placed the proton initially at a center of a cluster containing 512 water molecules.³⁰ In these and in subsequent calculations³¹ on cubic ice, water desorption was not found to occur.

The aim of the present work was to determine the sticking of H^+ and the water desorption probabilities for H^+ scattering from the basal plane (0001) face of hexagonal ice at normal incidence, for low E_i (0.05–4 eV) and $T_s = 80$ K, the latter value being intermediate to temperatures in the stratosphere and the ISM, using the CT method. The use of classical mechanics for our purpose can be justified on the basis that Ohmine and co-workers observed water desorption from amorphous ice clusters at an early stage directly following impact, where the proton transfer can be assumed to occur in a classical regime.¹⁰ We have found significant probabilities for collision induced desorption, even at the lowest E_i studied. Surprisingly, we also found high proton reflection probabilities at low E_i (0.4 at $E_i = 0.05$ eV), even though adsorbed protons have a very strong interaction with ice. We have also studied the binding energy of the proton adsorbed to ice.

The rest of this paper is structured as follows. Section 2 describes the method used, with respect to the treatment of the ice surface (section 2.1) and the proton interacting with it (section 2.2). The results are presented and discussed in section 3, where section 3.1 focuses on the sticking and the subsequent interaction of the proton with the water molecules. Section 3.2 provides a brief discussion of the surprising reflection observed at low E_i , and section 3.3 discusses collision induced desorption of the water molecules. Finally, section 4 concludes.

2. Method

To simulate the interaction between H^+ and the (0001) surface of ice I_h , the CT method³² was used, essentially following the same approach as used before to study the sticking of HCl and CO to ice surfaces.^{33–35}

2.1. Ice Surface. The ice surface was simulated using the molecular dynamics (MD) method.³⁶ The surface consists of 360 water molecules, distributed over four bilayers of moving molecules superimposed on two fixed bilayers (60 water molecules per bilayer). Periodic boundary conditions were applied in the x and y directions parallel to the surface, to simulate an infinite surface. The water molecules in the moving bilayers were treated as rigid rotors but were otherwise allowed to move according to Newton's equations of motion. Obviously, the rigid rotor approximation implies that the existing OH bonds cannot be broken. This constraint is justified to the extent that water molecules were *only* observed to break into fragments by ion bombarding at incidence energies that are at least an order of magnitude higher than those used in our calculations.^{4,8,28} The rigid rotor approximation also implies that anomalous proton diffusion (H_3O^+ transfers another proton to a neighboring water molecule than the proton originally transferred to it) cannot be modeled. The implications of that will be discussed below.

The initial configuration of the ice surface obeyed the ice rules³⁷ and had a zero dipole moment. To simulate the interactions between the water molecules, the TIP4P pair potential³⁸ was used:

$$V_{w-w} = LJ_{O-O}(12 - 6) + \sum_{i,j=1}^3 \frac{q_i q_j}{r_{ij}} \quad (1)$$

where the first term is the Lennard-Jones potential³⁹ centered on the oxygen atoms. It represents the Pauli repulsion and dispersion interactions between two water molecules. The second term represents the electrostatic energy, where q_i and q_j are the charges of the two water molecules, separated by r_{ij} . In this model, two positive charges are on the water hydrogen atoms and a third negative charge is at a distance of 0.15 \AA from the oxygen atom, along the bisector of the HOH angle. The surface was equilibrated at $T_s = 80$ K, using a computational analogue of a thermostat.⁴⁰ The thermostat was applied for 20 ps, and the surface was then left to equilibrate for a further 100 ps, using a time step of 1 fs. We do not expect any dependence of the results obtained here on T_s because of the strong binding energy of the proton to the surface, similar to our finding in the case of HCl sticking to ice,³⁴ whereas a dependence on T_s was evident in the case of H-atoms sticking to ice, the interaction of neutral H-atoms with ice being very weak.⁴¹

Top and side views of the (0001) basal plane ice surface are shown in Figure 1a and b, respectively. In the ice surface, the water molecules are arranged in chair shaped hexagonal rings in each bilayer (two monolayers per bilayer, separated by about 1 \AA) as shown in Figure 1a. These hexagonal rings are superimposed on each other, forming shafts running normal to the scattering surface. The water molecules in the topmost monolayer at the surface vacuum interface are three-coordinated; i.e., forming three hydrogen bonds with the neighbouring water molecules in the second monolayer of the same bilayer. The topmost monolayer molecules are of two classes. In the first, a water molecule has one of its protons upward pointing to the gas phase, away from the surface, and the second proton points down obliquely, forming a hydrogen bond with a water molecule in the second monolayer. A

(32) Porter, R. N.; Raff, L. M.; Miller, W. H., Eds. *Dynamics of Molecular Collisions, Part B*; Plenum: New York, 1976; p 1.

(33) Al-Halabi, A.; Kleyn, A. W.; Kroes, G. J. *J. Chem. Phys. Lett.* **1999**, *307*, 505.

(34) Al-Halabi, A.; Kleyn, A. W.; Kroes, G. J. *J. Chem. Phys.* **2001**, *115*, 482.

(35) Al-Halabi, A.; Kleyn, A. W.; van Dishoeck, E. F.; van Hemert, M. C.; Kroes, G. J. *J. Phys. Chem. A* **2003**, *107*, 10615.

(36) Allen, M. P.; Tildesley, D. J. *Computer Simulations of Liquids*; Clarendon: Oxford, 1987.

(37) Bernal, J. D.; Fowler, R. H. *J. Chem. Phys.* **1933**, *1*, 515.

(38) Jorgensen, W. L.; Chandrasekhar, J.; Madura, J. D.; Impey, R. W.; Klein, M. L. *J. Chem. Phys.* **1983**, *79*, 926.

(39) Lennard-Jones, J. E.; Devonshire, A. F. *Nature* **1936**, *137*, 1069.

(40) Berendsen, H. J. C.; Postma, J. P. M.; van Gunsteren, W. F.; DiNola, A.; Haak, J. R. *J. Chem. Phys.* **1984**, *81*, 3684.

(41) Al-Halabi, A.; Kleyn, A. W.; van Dishoeck, E. F.; Kroes, G. J. *J. Phys. Chem. B* **2002**, *106*, 6515.

(30) Kobayashi, C.; Saito, S.; Ohmine, I. *J. Chem. Phys.* **2000**, *113*, 9090.

(31) Kobayashi, C.; Saito, S.; Ohmine, I. *J. Chem. Phys.* **2001**, *115*, 4742.

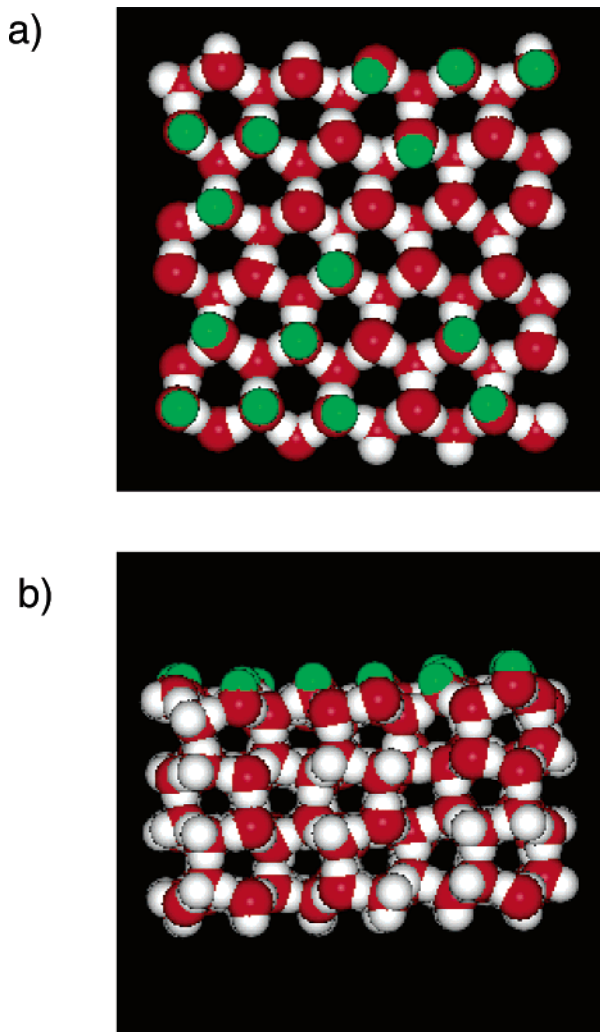


Figure 1. Top and side views of the crystalline ice surface. The green spheres show the dangling H-atoms. The red and white spheres represent the oxygen and the hydrogen atoms of the surface water molecules, respectively.

water molecule of the second class has both its protons pointing obliquely downward, forming hydrogen bonds with two neighbouring water molecules in the second monolayer. The water molecules in the second monolayer and below are four-coordinated, i.e., forming four hydrogen bonds.

2.2. Impinging Proton. The interaction between the proton and the ice surface was computed as a sum over pair potentials describing the interaction between the proton and individual water molecules. The proton–water interaction has the form⁴²

$$V_{w-H^+} = \sum_{i=1}^3 \left[\frac{q_i e}{r_i} + C/r_i^9 \delta_{i3} \right] \quad (2)$$

where the first term represents the electrostatic interactions between the proton of charge e and the charges q_i on the water molecule, r_i being the separation between the proton and q_i . The second term is a hard-core repulsive potential, which is present because the proton starts to acquire a cloud of negative charge as it approaches the water molecule. In the hard-core part, C is equal to $9.04 \text{ eV } \text{\AA}^9$ ($872.4 \text{ kJ/mol } \text{\AA}^9$), the Kronecker delta (δ_{i3}) term signifying that this repulsive interaction acts between the proton and the site of the negative charge on the water molecule only. This pair potential has been used in several

studies to investigate proton hydration.^{43,44} The binding energies and the distances between the proton and the water oxygen atoms in small clusters calculated using the interaction potential described in eq 2 agree well with ab initio results⁴⁵ and with experimental data (ref 46 and 42 and references therein). For instance, the model yields a proton–single water molecule interaction energy of 7.3 eV ,⁴² in good agreement with the experimental value 7.2 eV .⁴⁷

In the CT calculations presented here, the Monte Carlo technique was used to choose at random the initial impact position of the impinging proton on the ice surface. Three hundred trajectories were run for different values of E_i ranging from 0.05 to 4 eV , at normal incidence. Each trajectory was run for 5 ps , focusing on the initial interaction of the proton with the ice. A time step of 0.05 fs was employed. At the beginning of each trajectory, the proton was placed 11.3 \AA above the ice surface. In the MD simulations and in the simulations of the proton–ice collision dynamics, Newton’s equations of motion of the proton and the water molecules were integrated using an improved leapfrog algorithm.⁴⁸ In the CT calculations, the proton– H_2O interaction is switched off between 9.5 and 10 \AA , using a switching function.⁴⁹ As will be described below, we tested whether this procedure affects the calculations of the sticking probability, at the lowest collision energy we considered.

The ice surface was operationally defined to be at a height of 22.5 \AA , with $Z = 0$ being the position of the lowest static bilayer of the simulated ice slab. The sticking of the proton was defined to occur if the trajectory exhibited more than one turning point in the Z coordinate of the H^+ , such that, at the end of the trajectory, H^+ ends on top of or in the ice surface. For each value of E_i , the sticking probability (P_S) is defined as the number of sticking trajectories divided by the total number of trajectories (300). The estimated standard deviation of P_S is calculated as one standard deviation.^{50,51} The second possibility is that the proton scatters back to the gas phase, which is operationally defined to occur if the proton–surface distance becomes 7 \AA after the impact with the surface. Surface penetration by H^+ has also been studied by looking at the final position of the H^+ with respect to the ice surface at the end of the sticking trajectories. Surface penetration is defined to occur if the final position of the stuck proton is below 22.5 \AA , similar to the definition used to study HCl penetration into crystalline ice.³³ In the analysis, we have also considered the final position of the proton with respect to the surface bilayers and the possible formation of proton–water complexes that occurs after trapping. Finally, we have also considered the water desorption from the ice surface that occurs upon the collision of the proton with the surface.

In our study of the dynamics of the interaction of the proton with ice, the two major approximations are the use of classical mechanics and the use of the rigid rotor model for the water molecules. The validity of these approximations is best judged in the light of the two major findings of this study: the significant reflection probabilities at low incidence energies and significant probabilities for collision induced desorption (see below). We believe that neither approximation affects the calculation of the reflection probability, the observed reflection occurring from barriers that are due to electrostatic interactions and that are too high and too broad for the reflection to be affected by tunneling.

The situation with respect to collision induced desorption is more complicated. The classical calculations of Ohmine and co-workers show

- (43) Kozack, R. E.; Jordan, P. C. *J. Chem. Phys.* **1993**, *99*, 2978.
 (44) Svanberg, M.; Pettersson, J. B. C. *J. Phys. Chem. A* **1998**, *102*, 1865.
 (45) Valeev, E. F.; Schaefer, H. F., III *J. Chem. Phys.* **1998**, *108*, 7197.
 (46) Dalleska, N. F.; Honma, K.; Armentrout, P. B. *J. Am. Chem. Soc.* **1993**, *115*, 12125.
 (47) Goebbert, D. J.; Wenthold, P. G. *Euro. J. Mass. Spectrom.* **2004**, DOI 10.1255/ejms.684.
 (48) Fincham, D. *Mol. Simul.* **1992**, *8*, 165.
 (49) Kroes, G. J.; Clary, D. C. *J. Phys. Chem.* **1992**, *96*, 7079.
 (50) Gardner, D. O. N.; Al-Halabi, A.; Kroes, G. J. *J. Phys. Chem. B* **2004**, *108*, 3540.
 (51) Hays, W. L. *Statistics*; Holt-Saunders: New York, 1981.

(42) Kozack, R. E.; Jordan, P. C. *J. Chem. Phys.* **1992**, *96*, 3131.

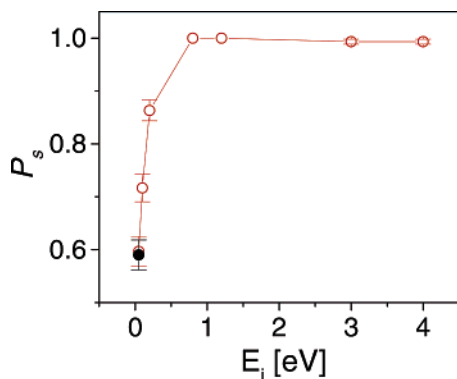


Figure 2. Sticking probability of H^+ to crystalline ice plotted as a function of E_i , for normal incidence at $T_s = 80$ K (open circles). For each E_i , 300 trajectories were run. The error bars in the figure represent one standard deviation. The solid circle represents P_s computed for $E_i = 0.05$ eV and switching off the proton–water interaction for $\text{H}^+ - \text{H}_2\text{O}$ distance between 14.0 and 14.5 Å (see the text for more details).

that it occurs at the onset of proton absorption, during which time proton transfer is classical to the extent that the energy of the transferred proton is higher than the barrier over which it is transferred,¹⁰ justifying the use of classical mechanics. On the other hand, during this time the proton transfer often occurs through the “anomalous” mechanism referred to above, accompanied by energy transfer to intramolecular vibrations. It is therefore possible that the collision induced desorption is affected by the anomalous proton diffusion mechanism and the energy transfer to the intramolecular vibrations that could accompany it. Because the transfer of energy from the incident proton to the high frequency intramolecular vibrations can probably not be modeled reliably with classical mechanics and fully quantum mechanical simulations of protons colliding with flexible, quantum dynamical water molecules and leading to collision induced desorption are outside the scope of our possibilities, the decision was made to perform the classical simulations within the rigid rotor approximation for the water molecules. We believe that, even with the approximate nature of the model used, the predictions made below of significant probabilities of proton reflection and collision induced desorption of water molecules from ice at low incidence energies are of high enough interest to stimulate experimental efforts aimed at validation.

3. Results and Discussion

3.1. Sticking. Figure 2 shows the computed P_s of H^+ to the ice surface as a function of E_i . At low values of E_i (up to 0.8 eV), P_s increases substantially with E_i . This is in contrast to what one would expect, as a larger amount of energy has to be transferred to the surface for sticking to occur at higher values of E_i . Previous computer simulations performed to study the interaction of HCl, CO, and H_2 molecules with crystalline and amorphous ice^{33,35,52,53} showed that P_s decreases with E_i , in agreement with experiments performed on HCl, N_2 , and H_2 scattering from ice.^{53–56} Because the binding energy of the trapped proton (see below) is much higher than the values of E_i considered here, one might expect a high P_s (approximately unity) for all values of E_i studied here. The increase of P_s with E_i observed here for $E_i \leq 0.8$ eV arises from the proton

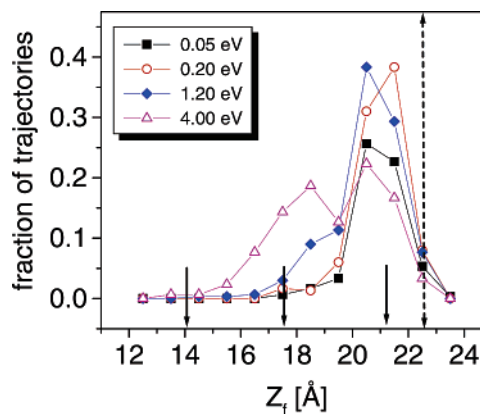


Figure 3. Fraction of sticking trajectories plotted for four different E_i , according to Z_i of H^+ at the end of the trajectories, for normal incidence at $T_s = 80$ K. For each E_i , 300 trajectories were run. The positions of the surface bilayers are shown by the arrows at the bottom of the figure. The surface–vacuum interface, indicated by the dashed long double arrow, is located at 22.5 Å, with $Z = 0$ defined as the bottom of the ice slab, including the fixed two bilayers.

encountering, at particular impact points, a repulsive barrier that it cannot overcome, due to its interaction with the positive charges of upward pointing hydrogen atoms of surface molecules (see below for more details). As discussed in section 2.2, we tested whether the high reflection probability obtained for low E_i was not an artifact of switching off the $\text{H}^+ - \text{H}_2\text{O}$ potential at $\text{H}^+ - \text{H}_2\text{O}$ distances of 9.5–10.0 Å. For this purpose, 300 additional trajectories were run at the lowest E_i (0.05 eV), switching off the $\text{H}^+ - \text{H}_2\text{O}$ interaction between 14 and 14.5 Å and initiating the trajectory at a distance of 16.5 Å from the surface. These additional calculations predict a value of P_s that agrees with the one previously computed to within the statistical error (see Figure 2). The high reflection probabilities predicted here are thus not an artifact of using a short ranged potential. Instead, they represent results of dynamics calculations using a realistic model potential that can be tested by ion scattering experiments.

For high energies (≥ 1 eV), P_s converges to 1, as shown in Figure 2. The apparent decrease in P_s at $E_i > 0.8$ eV is not statistically significant with the number of the trajectories that has been run. The high P_s values at high energies found here are in qualitative agreement with the findings of the ion scattering experiments of Souda,⁷ performed at incidence energies (100 eV) that are about 2 orders of magnitude higher than those considered here.

For most of the sticking trajectories, we find that the stuck proton is absorbed inside the ice surface; i.e., the proton penetrates the ice even at the lowest values of E_i (Figure 3). At low values of E_i , Figure 3 shows that the protons are stuck to the surface mainly in the first bilayer or between the first and second surface bilayers. However, at higher E_i some protons penetrate deeper (in some cases about 10 Å) into the second or third bilayer (Figure 3); i.e., the proton penetration depth increases with E_i . This is in agreement with the results of CT calculations of O^+ scattering from cubic ice,⁸ where most of the impinging O^+ ions were found to be implanted rather than reflected at energies higher than those considered here ($E_i = 23–115$ eV). Our finding that the proton may penetrate the ice surface by as much as 10 Å suggests that experiments on penetration of ice by protons could yield information on surface disorder and surface melting at low E_i (as low as 3 eV). In the

(52) Al-Halabi, A.; Fraser, H. J.; Kroes, G. J.; van Dishoeck, E. F. *Astron. Astrophys.* **2004**, *422*, 777.

(53) Hornekaer, L.; Baurichter, A.; Petrunin, V. V.; Luntz, A. C.; Kay, B. D.; Al-Halabi, A. *JCP*, submitted.

(54) Andersson, P. U.; Näägård, M. B.; Bolton, K.; Svanberg, M.; Petterson, J. B. C. *J. Phys. Chem. A* **2000**, *104*, 2681.

(55) Andersson, P. U.; Näägård, M. B.; Petterson, J. B. C. *J. Phys. Chem. B* **2000**, *104*, 1596.

(56) Gotthold, M. P.; Sitz, G. O. *J. Phys. Chem. B* **1998**, *102*, 9557.

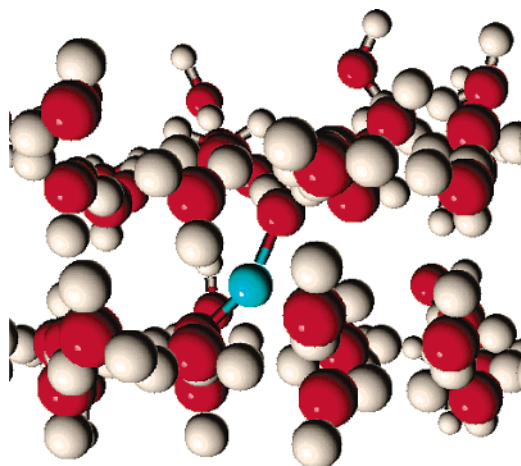


Figure 4. A side view showing the Zundel complex of the trapped proton (indicated by the blue sphere) interacting with two surface water molecules in two different surface bilayers, for normal incidence at $T_s = 80$ K.

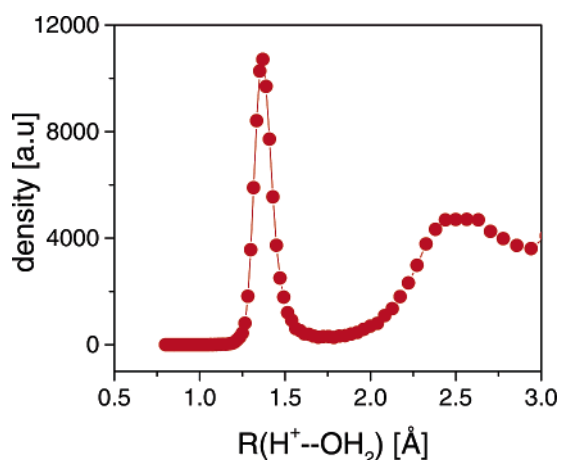


Figure 5. A distribution of the oxygen-proton distance is shown for all the sticking trajectories for normal incidence, at $E_i = 4.0$ eV and $T_s = 80$ K.

past, proton scattering experiments have probed the surface melting of ice at much higher incidence energies (100 keV), observing backscattered protons.⁵

In most cases of sticking, independent of the value of E_i , we found that H^+ interacts strongly with two water molecules forming the well-known Zundel complex ($H_5O_2^+$), as illustrated in Figure 4, rather than forming a hydronium ion, as observed in simulations on proton solvation in large water clusters, using the same potential we have used here.^{43,44} The figure shows the configuration of a complex, in which the proton interacts with two water molecules in two different surface bilayers. In this configuration, the proton is approximately equidistant (1.3–1.4 Å) from the O-atoms of the two water molecules forming the complex. In Figure 5, a distribution function of $R(O-H^+)$, the distance between the proton and the oxygen atom of each water molecule, is plotted for all the sticking trajectories at $E_i = 4.0$ eV. The first peak at about 1.4 Å corresponds to the Zundel complex. The same distributions were found for other values of E_i , as would be expected. The H^+-O distance of 1.4 Å is in reasonable agreement with that (1.3 Å) obtained from calculations of proton solvation in water using the ab initio molecular dynamics method.^{57,58} The latter value is somewhat larger still than that found for the Zundel complex in the gas phase, where the distance is about 1.2 Å.^{59,60} These differences

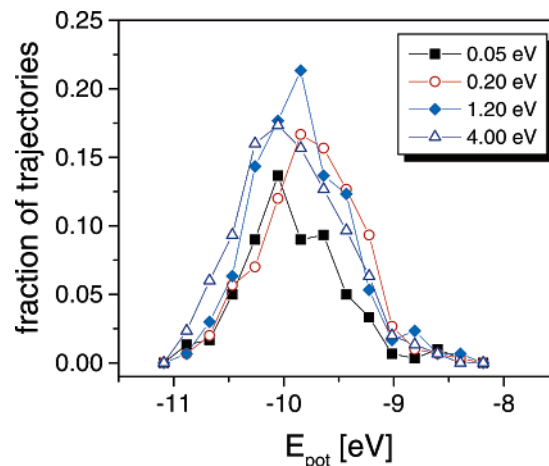


Figure 6. Fraction of the sticking trajectories plotted as a function of the potential energy of H^+ at the end of the trajectories for four values of E_i , for normal incidence at $T_s = 80$ K. For each E_i , 300 trajectories were run.

probably arise from the water molecules in the ice surface being less free to rearrange their position than those in liquid water and in small water clusters.

In Figure 6, distributions of the final proton potential energies (binding energies) for the sticking trajectories are shown for four values of E_i . The distributions are very similar for all E_i . The average binding energy of the trapped proton calculated from all sticking trajectories is found to be 9.9, and the standard deviation is 0.5 eV. The computed average binding energy is independent of the value of E_i (Figure 6), suggesting that the proton-ice system achieves equilibrium within 5 ps. One can compare the calculated proton binding energy we obtained with the proton solvation enthalpy, taking into account that the volume change is not significant in our calculations. The measured proton solvation enthalpy in liquid water is about 11.9 eV,⁶¹ in reasonable agreement with our calculated value (9.9 eV). The calculated interaction energy of H_3O^+ with cubic ice (5.9 eV) calculated by Ohmine and co-workers^{30,31} corresponds to a proton binding energy of 12.5 eV, by using eq 8 of ref 61, which relates the proton binding energy with that of H_3O^+ in liquid water. This value is also in fair agreement with our calculated value.

3.2. Scattering. The scattering of protons from ice is most likely to occur at low values of E_i (≤ 0.2 eV) as shown in Figure 2. To understand the scattering dynamics, we have examined in more detail the scattering trajectories. Two typical types of collisions that result in scattering were found. In the first case, H^+ is scattered back when it collides with a surface hexagonal ring that contains three water molecules in the topmost monolayer (see Figure 1) whose hydrogen atoms are upward pointing, away from the ice surface. In the second situation, H^+ is directly scattered from a single upward pointing hydrogen atom. The scattering occurs due to a rather localized electrostatic repulsive interaction between the charge of the proton and the charges of the water hydrogen atoms. At these low values of

(57) Tuckerman, M.; Laasonen, K.; Sprik, M.; Parrinello, M. *J. Chem. Phys.* **1995**, *103*, 150.

(58) Marx, D.; Tuckerman, M. E.; Hutter, J.; Parrinello, M. *Nature* **1999**, *397*, 601.

(59) Ojamäe, L.; Shavitt, I.; Singer, S. J. *J. Chem. Phys.* **1998**, *109*, 5547.

(60) Auer, A. A.; Helgaker, T.; Klopper, W. *Phys. Chem. Chem. Phys.* **2000**, *2*, 2235.

(61) Coe, J. V.; *Chem. Phys. Lett.* **1994**, *229*, 161.

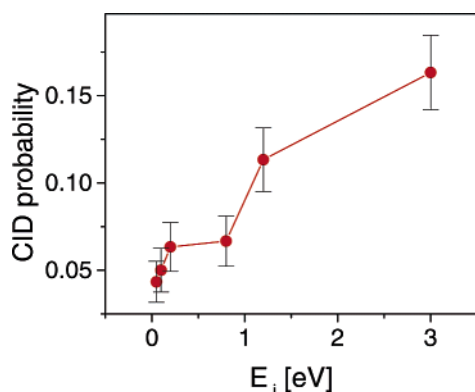


Figure 7. Probability of CID shown as a function of E_i , for normal incidence at $T_s = 80$ K. For each E_i , 300 trajectories were run. The error bars in the figure represent one standard deviation.

E_i , the molecule is scattered at distances between 5 and 9 Å from the top surface bilayer. At high values of E_i , a few scattering trajectories were found to occur in which the reflection was due to the interaction with the hard-core potential in addition to the electrostatic repulsion (the proton was scattered very close to the atoms of the water molecules in the top bilayer). In all cases, the scattering of the proton was observed to occur immediately upon impact.

3.3. Collision Induced Desorption of Water Molecules.

Upon impact of the proton, even at the lowest E_i some water molecules are “puffed” and attempt to leave the surface as observed in several trajectories. A water molecule is operationally defined to show collision induced desorption (CID) if its distance to the surface becomes larger than 7 Å; i.e., the same definition used to define proton reflection discussed in section 2.2. Here, we use the term “puffing” and CID rather than “sputtering” because, especially at the lowest E_i , the energy required for water desorption, which exceeds 30 kJ/mol, does not come from the initial collision energy but rather from the strong interaction of the proton with the nearest water molecules: the entering proton acts like a “Coulomb bomb”, triggering a local rupturing of the soft hydrogen bonding network by reorienting the water molecules close to it. Thus, it can happen that a surface water molecule suddenly finds that some of its neighbors, by reorienting, now repel it to the extent that the surface molecule can be thrown out.

The probability of CID is shown as a function of E_i in Figure 7. The probability increases with E_i , either because the proton’s excess energy is somehow dissipated directly to surface water molecules or because the proton’s excess energy allows the proton to enter places where it can more effectively disrupt the hydrogen bonding network. The importance of the charge-dipole induced rupture of the hydrogen bonding network in causing water desorption is underlined by the fact that no collision induced water desorption was found in CT calculations of scattering of polar molecules such as HCl³⁴ or HF⁶² from ice, at collision energies as high as 2 and 1 eV, respectively. The importance of this mechanism also suggests that the influence of incidence angle and T_s on the CID probability will be small. More details will be published elsewhere.⁶³

In nearly all CID trajectories, *only* a single water molecule desorbs from the surface, while in only a very few cases is a second water molecule ejected from the surface. However, this second molecule is always readsorbed, returning to the surface because it does not have enough kinetic energy to escape from the surface. Also, in nearly all CID trajectories, the puffed water molecules come from the surface–vacuum interface; i.e., they are three-coordinated water molecules (see section 2.1 for details) in the top surface monolayer, in agreement with experimental studies of H⁺–ice collisions at high energies^{6,4} and theoretical studies of O⁺–ice collisions at hyperthermal energies.⁸

We cannot perform a quantitative comparison of our results with the previous CT calculations of ref 9 on collision induced water desorption from amorphous ice clusters, because very few (up to 5 per E_i) trajectories were computed in that work. At low values of E_i (as low as 0.000 84 eV), these calculations showed that more than one water molecule per trajectory desorbed from a water cluster. Water desorption was found to be quite efficient for all trajectories at all energies considered in their study (except at $E_i = 210$ and 840 eV). Similar results were obtained in the explorative classical calculations (20 trajectories) by Ohmine and co-workers¹⁰ on proton attachment to cold water clusters, where 3.8 water molecules were desorbed on average per trajectory. The discrepancies between our findings and those for amorphous ice (cold water) clusters can be explained from the differences in the nature of the ice surfaces, in particular, the binding energies of the surface water molecules at the proton impact sites. The amorphous water clusters used were small, consisting of 100⁹ and 64¹⁰ water molecules. The surfaces of those clusters are very irregular, and many surface molecules have a low hydrogen bond coordination number (as shown in simulations of amorphous water clusters by Buch;⁶⁴ see also ref 65 for more details). In contrast, our crystalline ice surface is much more regular, with the water molecules at the surface being coordinated by three or four other water molecules. Because water evaporation should be the easier the less tightly bound a surface molecule is, evaporation of more molecules can be expected from amorphous ice clusters.

Finally, in our calculations, desorption of water molecules occurs within the first picosecond following proton impact, in agreement with the observation of fast water desorption (within 0.8 ps) in the calculations of Ohmine and co-workers.¹⁰ The water erosion thus occurs during the initial interaction of the proton with the ice surface, i.e., during the time that classical mechanics is expected to yield a good description of the proton’s motion in the ice¹⁰ (see also section 2.2).

4. Conclusions

In this paper, we have presented the results of CT calculations on the sticking of H⁺ to the basal plane (0001) of crystalline ice, for collision energies from 0.05 to 4.0 eV, at normal incidence for $T_s = 80$ K. A surprising prediction from our simulations is that the reflection probability is substantial at low values of E_i ($E_i \leq 0.2$ eV). In the case of reflection, the proton is scattered at a long distance from the ice surface, due to a repulsive electrostatic interaction with one or more upward

(62) Gardner, D. O. N.; Al-Halabi, A.; Kroes, G. J. *J. Chem. Phys.* **2004**, *120*, 11796.

(63) Al-Halabi, A.; Sanfelix, P. C.; Darling, G. R.; Holloway, S.; Kroes, G. J. To be submitted.

(64) Buch, V. *J. Chem. Phys.* **1992**, *96*, 3814.

(65) Al-Halabi, A.; van Dishoeck, E. F.; Kroes, G. J. *J. Chem. Phys.* **2004**, *120*, 3358.

pointing hydrogen atoms of the nearest water molecules in the first surface monolayer. The calculations predict that the reflection efficiency decreases with increasing E_i , P_s becoming essentially 1 at $E_i = 0.8$ eV and remaining 1 for all higher E_i values studied here. We hope that the predicted dependence of P_s can be confirmed experimentally, using thermal and hyperthermal incident protons scattering from crystalline ice.

In the case of sticking, H^+ penetrates the ice surface in most of the trajectories, even at low values of E_i . The penetration depth of the trapped proton increases with E_i . For most sticking trajectories, the proton interacts mainly with two water molecules, forming a Zundel cation ($H_5O_2^+$), rather than a H_3O^+ . The average proton–ice interaction energy was computed to be 9.9 eV with a standard deviation of 0.5 eV, in fair agreement with the measured and calculated binding energies of protons solvated in cubic ice^{30,31} and in water clusters.^{61,10} The proton was found to be approximately equidistant (1.4 Å) from the two oxygen atoms of the water molecules belonging to the Zundel complex.

Collision induced desorption of water upon proton impact has been observed even at the lowest E_i , increasing in efficiency

with E_i . In all CID trajectories, a single water molecule per trajectory is found to desorb and leave the surface, in agreement with the results of previous experiments on H^+ sticking to ice at high energies (MeV) and calculations on O^+ sticking to ice at hyperthermal energies (23–115 eV) (see also ref 4 and references therein). Exploratory calculations on proton association with small, cold water clusters found higher probabilities for CID and desorption of more molecules per trajectory, presumably because such clusters have more weakly bound water molecules at their surface than crystalline ice.^{9,10} The desorbed water molecule initially was always a part of the surface top monolayer at the surface–vacuum interface, i.e., a three-coordinated molecule in the top surface monolayer.

Acknowledgment. P.C.S. acknowledges the financial support from the EU-TMR Network on Surface Photochemistry under Contract No. ERB FMRX-CT98-0249 and EPSRC Grant GR/S15990. Part of the calculations were done with computing time funded by NCF (Netherlands Computing Facilities Foundation).

JA040171U